

Accepted Manuscript

Antibacterial and anti-TB tat-peptidomimetics with improved efficacy and half-life

Govind S. Bhosle, Laxman Nawale, Amar M. Yeware, Dhiman Sarkar, Moneesha Fernandes



PII: S0223-5234(18)30373-8

DOI: [10.1016/j.ejmech.2018.04.039](https://doi.org/10.1016/j.ejmech.2018.04.039)

Reference: EJMECH 10388

To appear in: *European Journal of Medicinal Chemistry*

Received Date: 22 December 2017

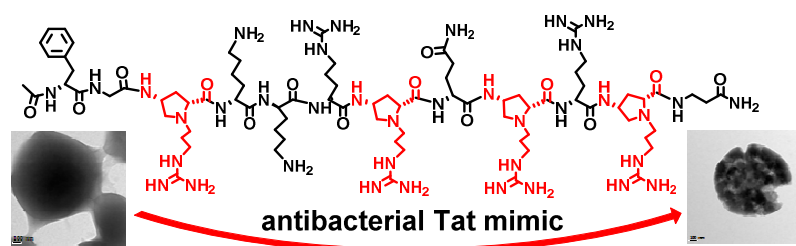
Revised Date: 15 March 2018

Accepted Date: 18 April 2018

Please cite this article as: G.S. Bhosle, L. Nawale, A.M. Yeware, D. Sarkar, M. Fernandes, Antibacterial and anti-TB tat-peptidomimetics with improved efficacy and half-life, *European Journal of Medicinal Chemistry* (2018), doi: 10.1016/j.ejmech.2018.04.039.

This is a PDF file of an unedited manuscript that has been accepted for publication. As a service to our customers we are providing this early version of the manuscript. The manuscript will undergo copyediting, typesetting, and review of the resulting proof before it is published in its final form. Please note that during the production process errors may be discovered which could affect the content, and all legal disclaimers that apply to the journal pertain.

Graphical Abstract



Antibacterial and anti-TB Tat-peptidomimetics with improved efficacy and half-life

Govind S. Bhosle,^[a,c] Laxman Nawale,^[b] Amar M. Yeware,^[b,c] Dhiman Sarkar^[b,c] and Moneesha Fernandes*^[a,c]

^[a] Organic Chemistry Division, CSIR-National Chemical Laboratory (CSIR-NCL), Dr. Homi Bhabha Road, Pune 411008, India. E-mail: m.dcosta@ncl.res.in

^[b] CombiChem-Bio Resource Center, Organic Chemistry Division, CSIR-National Chemical Laboratory (CSIR-NCL), Dr. Homi Bhabha Road, Pune 411008, India

^[c] Academy of Scientific and Innovative Research (AcSIR), CSIR-NCL Campus, Pune, India

Keywords: Non-natural amino acid • Tat-peptide • anti-bacterial • anti-TB • *Mycobacterium tuberculosis*

Abstract: Non-natural antimicrobial peptides are ideal as next generation antibiotics because of their ability to circumvent the problems of drug resistance and *in vivo* instability. We report novel all- α - and α,γ -mixed Tat peptide analogues as potential antibacterial and anti-TB agents. These peptides have broad spectrum antibacterial activities against Gram-positive (MICs 0.61 ± 0.03 to 1.35 ± 0.21 μM with the peptide γTatM4) and Gram-negative (MICs 0.71 ± 0.005 to 1.26 ± 0.02 μM with γTatM4) bacteria and are also effective against active and dormant forms of *Mycobacterium tuberculosis*, including strains that are resistant to rifampicin and isoniazid. The introduction of the non-natural amino acids of the study in the Tat peptide analogues results in increased resistance to degradation by proteolysis, significantly increasing their half-life. The peptides appear to inhibit bacteria by a membrane disruption mechanism, and have only a low cytotoxic effect on mammalian cells.

Introduction

Antimicrobial peptides (AMPs) act either by interacting with the cell membrane and causing lysis and ultimately cell death, or after penetrating the cell membrane, upon interaction with intracellular components,¹ in contrast to conventional drugs that typically act through inhibition of metabolic processes. Such peptides thus offer an opportunity to overcome the problem of resistance development, which is increasingly being encountered, and that makes diseases such as those caused by *Mycobacterium tuberculosis* (Mtb) and other pathogenic bacteria difficult to treat. To improve the stability to enzymatic hydrolysis and to increase bioavailability, several synthetic, non-natural AMPs² and mimetics have been reported.³ Many AMPs have a helical component that has been shown to be necessary for their antimicrobial activity. Among these, recently, Nepal *et al.*⁴ described cationic and amphiphilic proline-rich polyproline type II (PPII) helices for effective cell penetration of macrophages that also exerted potent antibacterial activity. PPII⁵ and other helical peptides such as 12-helical β -peptides have been reported by several groups to have varying degrees of antimicrobial activities,⁶⁻⁸ including against some species that are resistant to common

antibiotics such as vancomycin or penicillin.⁸ Several other groups have reported peptoids,⁹ α -aminoxy-peptides,¹⁰ α/β -peptides,^{11,12} or azapeptides,^{13,14} as synthetic mimics of AMPs.

We chose to study the effect of non-natural amino acid surrogates on the antibacterial properties of the Tat(48-57) peptide. The basic translocating region (48-60) of the trans-activating transcriptional activator (TAT) peptide,¹⁵ derived from the human immunodeficiency virus 1 (HIV-1) tat protein is a positively charged peptide, rich in arginine, and is highly studied for cell penetration and delivery of a variety of cargo molecules.¹⁶⁻¹⁹ The presence of several arginine residues, in addition to lysine residues, makes it particularly susceptible to the degradative action of enzymes, precluding its possible application in biological systems. Several reports of modifications in the Tat peptide have appeared in literature, where non-natural amino acids²⁰ as well as backbone linkages^{21,22} have been explored in relation to cell penetration. They have, however, not been studied for antimicrobial activity. There have appeared few reports²³⁻²⁸ of the antibacterial properties involving the cell-penetrating Tat peptide that involved the use of Tat peptide dimers,²³ Tat peptide-porphyrin conjugates,²⁵ D-Tat²⁶ (with D-amino acids instead of L-amino acids) and cholesterol-conjugated Tat peptides,²⁷ besides the Tat peptide itself,²⁶ that were shown to form nanoparticles and one report of its antifungal activity against human pathogenic fungi.²⁸ Studies with model membranes^{23,24} suggested that membrane disruption was the mode of antibacterial action of the cell-penetrating Tat peptide. By using transmission electron microscopy, we show that this is indeed the case. To our knowledge, there are no reports yet demonstrating the activity of the Tat peptide against mycobacteria, specifically *Mycobacterium tuberculosis* (Mtb). We report herein, the antibacterial and anti-TB effects of novel synthetic analogues of the Tat(48-57) peptide (GRKKRRQRRR). Their microcidal effect was envisioned considering the amphipathicity, overall charge and possible interaction with bacterial cell membranes. The antimicrobial properties of the peptides are a consequence of the novel non-natural lysine or arginine surrogates. Their inclusion in the Tat peptide leads to enhanced antibacterial activity for many of the derived peptides and significantly superior anti-TB properties in all of the derived peptides. Moreover, we show that the Tat peptide analogues are effective against both active and dormant forms of Mtb and MDR-Mtb, making this a promising class of candidates for future development in the therapy of tuberculosis. The effect of the chiral monomers on structural pre-organization of the derived peptides is also investigated to determine if this, in turn, influences their antimicrobial activity. An additional advantage includes increased protease resistance, extending their half-life and enhancing their application potential in biological systems. The novel Tat peptide analogues may also be envisioned to overcome the limitation of bacterial resistance development that is frequently encountered in the use of antibiotics, since AMPs²⁹ are less likely to lead to development of resistance,³⁰ being known to act by targeting the microbial membranes,²⁶ rather than metabolic processes, as in the case of small molecule drugs.^{31,32}

Results and Discussion

Synthesis of precursors **X** and **Z** to amino acid surrogates *r*, *k* and P^g respectively

Our laboratory has earlier reported the use of *N*-(aminoalkyl)proline-derived compounds towards the synthesis of peptide nucleic acids,³³ cell-penetrating oligomers³⁴ and as anti-glycation agents.³⁵ The amino acid surrogates, (2*S*,4*S*)-4-amino-*N*1-(3-guanidinopropyl)-proline (*r*), (2*S*,4*S*)-4-amino-*N*1-(3-aminopropyl)-proline (*k*) and (2*S*,4*S*)-4-amino-proline (P^g) were derived from (2*S*,4*R*)-4-hydroxyproline through the orthogonally protected precursors **X** and **Z** depicted in Figure 1. The incorporation of precursor **X** in combination with α -amino acids during peptide synthesis leads to α,γ -peptides containing the residues *r* or *k*, while the incorporation of precursor **Z** leads to all- α -peptides containing the residue P^g respectively.

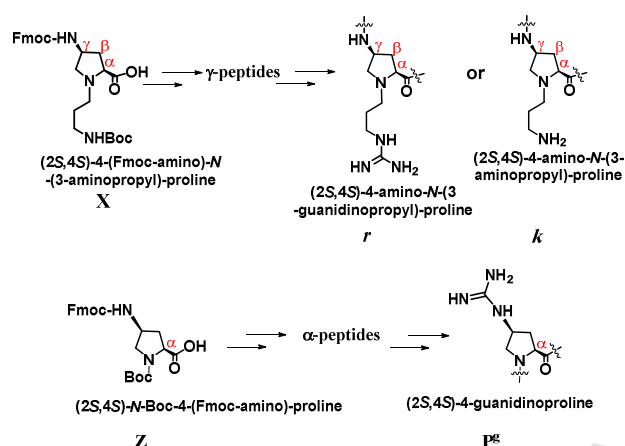
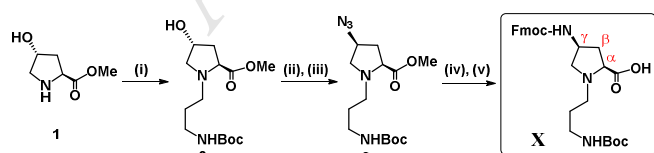


Figure 1. Amino acid surrogates- *r*, *k* and P^g , of the study.

Scheme 1 summarises the synthesis of protected non-natural amino acid **X**. The monomer was synthesized from commercially available *trans*-L-4-hydroxyproline. The hydroxyproline methyl ester **1** was *N*-alkylated upon reaction with 3-((*tert*-butyloxycarbonyl)amino)propyl methylsulfonate in the presence of triethylamine and catalytic amount of DMAP in DMF.³⁵ The 4-hydroxyl group in compound **2** was then converted to the azide **3** by mesylation, followed by S_N2 displacement of 4-*O*-mesyl group using NaN_3 in DMF. Catalytic hydrogenation of the azide group in **3** to the amine, followed by hydrolysis of the ester function and subsequent protection of the free amine using Fmoc-Cl and NaHCO_3 in dioxane: H_2O (1:1) yielded orthogonally protected non-natural amino acid **X**. A similar series of reactions was used to synthesize the orthogonally protected precursor **Z** to arginine surrogate P^g (Scheme S1, SI).



Scheme 1. Synthesis of orthogonally protected non-natural amino acid **X**. Reagents and conditions: (i) $\text{MsO}-(\text{CH}_2)_3\text{-NH-Boc}$, Et_3N , DMAP, DMF, 70°C , 62 % (ii) MsCl , Et_3N , CH_2Cl_2 , 73% (iii) NaN_3 , DMF, 65°C , 67 % (iv) (a) H_2 , Pd/C, MeOH, (b) LiOH, then HCl, 62

% for (a) and (b) (v) (a) Fmoc-Cl, NaHCO₃, H₂O-dioxane, (b) Dowex H⁺ resin, 58 % for (a) and (b).

Synthesis of Tat peptide analogues

The protected non-natural amino acids **X** and **Z** were used in the solid phase synthesis of Tat peptide derivatives. Peptides were assembled on MBHA resin by either Fmoc- or Boc-chemistry protocols. β -Alanine was coupled as the first amino acid as a spacer, followed by the coupling of other amino acids. All the coupling steps were done in dry DMF in presence of DIPEA, with HOBt and TBTU as coupling agents. Removal of the Boc-protecting group was achieved using 50% TFA in CH₂Cl₂, while the Fmoc group was removed using 20% piperidine in DMF. A phenylalanine residue was added at the N-termini of the peptides in order to facilitate concentration calculation from the UV absorbance. Guanidinylation of monomer **Z** to arginine surrogate **P^g** was performed on the solid support after *N*-acetylation of the phenylalanine residue at *N*-terminus, and removal of the Fmoc protecting group, using 1*H*-pyrazole-1-carboxamide hydrochloride and DIPEA in dry DMF. The synthesized peptides were cleaved from the resin by the TFA-TFMSA cleavage protocol and purified by RP-HPLC on a C18 column. Their purity was re-checked by analytical HPLC and all the peptides were characterized by MALDI-TOF analysis (SI). Table 1 lists the peptides synthesized, while the chemical structures are depicted of representative peptides in Figure 2 and of all peptides in the SI, pages S16 & S17. The peptides γ Tat1M and γ Tat1C (Table 1, entries 1 and 2 respectively) contain one *r* unit, either in the middle of the oligomer, or at the 'C'-terminal. Likewise, the α Tat1M and α Tat1C peptides (Table 1, entries 7 & 8 respectively) contain one **P^g** unit in the middle and 'C'-terminal positions respectively. γ TatM3, γ TatM3wg and α TatM3 peptides contain three units each of *r*, *k* or **P^g** respectively, distributed across the oligomer (Table 1, entries 3, 4 & 9 respectively), while γ TatM4, γ TatM4wg and α TatM4 peptides contain four units each of *r*, *k* or **P^g** respectively, distributed across the oligomer (Table 1, entries 5, 6 & 10 respectively). A control Tat peptide (ctrlTat) was also synthesized (Table 1, entry 11) for comparison.

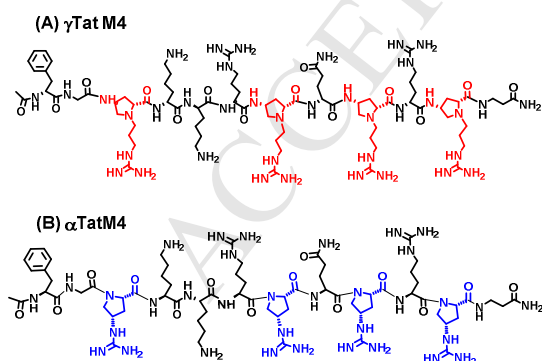


Figure 2. Representative Tat peptides of the study- (A) γ TatM4 and (B) α TatM4.

Table 1. Peptides of the study[#].

Entry	Code	Peptide sequence
-------	------	------------------

1	γ Tat1M	Ac-FGRKKrQRRR- β Ala-NH ₂
2	γ Tat1C	Ac-FGRKKRRQRRr- β Ala-NH ₂
3	γ TatM3	Ac-FGrKKRrQRRr- β Ala-NH ₂
4	γ TatM3wg	Ac-FGkKKRkQRRk- β Ala-NH ₂
5	γ TatM4	Ac-FGrKKRrQrRr- β Ala-NH ₂
6	γ TatM4wg	Ac-FGkKKRkQkRk- β Ala-NH ₂
7	α Tat1M	Ac-FGRKKP ^g RQRRR- β Ala-NH ₂
8	α Tat1C	Ac-FGRKKRRQRRP ^g - β Ala-NH ₂
9	α TatM3	Ac-FGP ^g KKRP ^g QRRP ^g - β Ala-NH ₂
10	α TatM4	Ac-FGP ^g KKRP ^g Q ^g RP ^g - β Ala-NH ₂
11	ctrlTat	Ac-FGRKKRRQRRR-NH ₂

r = (2S,4S)-4-amino-N-(3-guanidinopropyl)-proline, k = (2S,4S)-4-amino-N-(3-aminopropyl)-proline, P^g = (2S,4S)-4-guanidinoproline.

Antibacterial activity of the Tat peptide analogues of the study

The novel Tat peptides of the study were tested for antimicrobial activity against Gram-positive (*Staphylococcus aureus*, *Bacillus subtilis*, *Staphylococcus epidermidis*) and Gram-negative (*Escherichia coli*, *Pseudomonas aeruginosa*, *Enterobacter spp.*) bacteria. The data obtained are summarized as IC₉₀ or MIC values in Table 2. The IC₅₀ values are listed in the SI (Table S1).

Among all the peptides, the γ TatM4 peptide displayed the best activity, with the lowest IC₅₀ (SI, Table S1) and MIC values against Gram-positive as well as Gram-negative bacteria. Specifically, the MIC values for γ TatM4 against *E. coli*, *P. aeruginosa*, *Enterobacter spp.*, *S. aureus*, *B. subtilis* and *S. epidermidis* were 1.12, 0.61, 1.35, 1.26, 0.71 and 1.12 μ M respectively (Table 2).

Activity against *Mycobacterium tuberculosis*

The activity of the peptides of the study against Mtb and MDR-Mtb are depicted as their MIC values in Figure 3 and listed in Table 3. The corresponding IC₅₀ values are listed in the SI, Table S2. Against Mtb, γ Tat1M was the most active against the dormant and active forms (MIC 13.8 and 20.1 μ M respectively). Against MDR-Mtb, the γ TatM4wg and α TatM3 peptides showed the best activity, with MIC values of 6.6 μ M and 6.0 μ M respectively against the dormant form and 12.8 μ M and 15.0 μ M respectively, against the active form. The γ Tat1M peptide also showed moderate activity against MDR-Mtb, with MIC values of 10.6 μ M and 13.0 μ M against the dormant and active forms respectively.

Circular Dichroism studies

The CD spectra of the Tat peptides of the study were recorded in water as well as in presence of the secondary structure-inducing solvent, trifluoroethanol (TFE). The spectra are shown in Figure 5. The ctrlTat peptide study displayed a random coil structure in water, as reported

earlier,³⁶ but showed a significant change towards the α -helical structure in the presence of TFE (Figure 4 (a) and 4 (b)). A similar trend was observed for the all- α -peptides of this study. The α,γ -peptides, on the other hand, displayed differing CD signatures. The γ TatM4, γ TatM4wg and γ TatM3wg peptides were found to display markedly different CD signatures from the other α,γ -peptides. This trend was also found in these peptides in the presence of TFE. The γ Tat1C peptide was found to display a CD signature very similar to that of the ctrlTat peptide in TFE, and tending towards the signature observed for α -helices³⁷ in the case of α -peptides. Coincidentally, this peptide also had very similar antibacterial activity to the ctrlTat peptide against the bacteria tested, as evident from Figure 2.

Table 2. MIC data for peptides of the study against Gram-positive and Gram-negative bacteria.

Entry	MIC ^a (μ M) of peptides with SD (\pm)					
	Gram-negative			Gram-positive		
	<i>E. coli</i>	<i>P. aeruginosa</i>	<i>Enterobacter spp.</i>	<i>S. aureus</i>	<i>B. subtilis</i>	<i>S. epidermidis</i>
γ Tat1M	7.25 \pm 0.06	2.67 \pm 0.04	4.70 \pm 0.49	5.25 \pm 0.11	14.1 \pm 0.47	8.95 \pm 1.2
γ Tat1C	5.71 \pm 0.04	3.35 \pm 0.03	18.85 \pm 1.28	8.47 \pm 0.17	3.56 \pm 0.04	4.92 \pm 0.5
γ TatM3	7.58 \pm 0.03	1.82 \pm 0.005	8.01 \pm 0.58	9.05 \pm 0.33	2.81 \pm 0.02	9.44 \pm 0.82
γ TatM3wg	3.52 \pm 0.08	2.32 \pm 0.047	4.65 \pm 0.23	3.02 \pm 0.05	4.16 \pm 0.06	7.25 \pm 0.64
γ TatM4	1.12 \pm 0.01	0.61 \pm 0.03	1.35 \pm 0.21	1.26 \pm 0.02	0.71 \pm 0.005	1.12 \pm 0.23
γ TatM4wg	2.34 \pm 0.05	2.2 \pm 0.02	4.51 \pm 0.44	3.02 \pm 0.03	3.79 \pm 0.08	3.94 \pm 0.54
α Tat1M	13.49 \pm 0.02	6.53 \pm 0.42	nd	8.65 \pm 0.18	29.85 \pm 1.15	nd
α Tat1C	6.73 \pm 0.03	10.26 \pm 0.03	nd	10.95 \pm 0.66	7.96 \pm 0.12	nd
α TatM3	11.8 \pm 0.018	12.62 \pm 0.06	nd	20.54 \pm 0.85	13.2 \pm 0.54	nd
α TatM4	27.73 \pm 0.04	25.98 \pm 0.79	nd	5.59 \pm 0.42	15.13 \pm 0.73	nd
ctrlTat	6.27 \pm 0.05	7.46 \pm 0.69	21.60 \pm 1.95	9.91 \pm 0.25	3.34 \pm 0.04	5.78 \pm 0.51
Ampicillin ^b	4.17 \pm 0.036	12.5 \pm 0.09	nd	2.8 \pm 0.01	29.5 \pm 0.3	nd
Kanamycin ^b	3.3 \pm 0.024	1.01 \pm 0.06	nd	>61.9 \pm 0.6	2.8 \pm 0.027	nd

^a The values are expressed as the mean of triplicates. Antibacterial activity of each peptide was determined by serial dose dependent dilutions. ^b Standard antibacterial drug and positive control. SD (\pm) = standard deviation. nd = not determined.

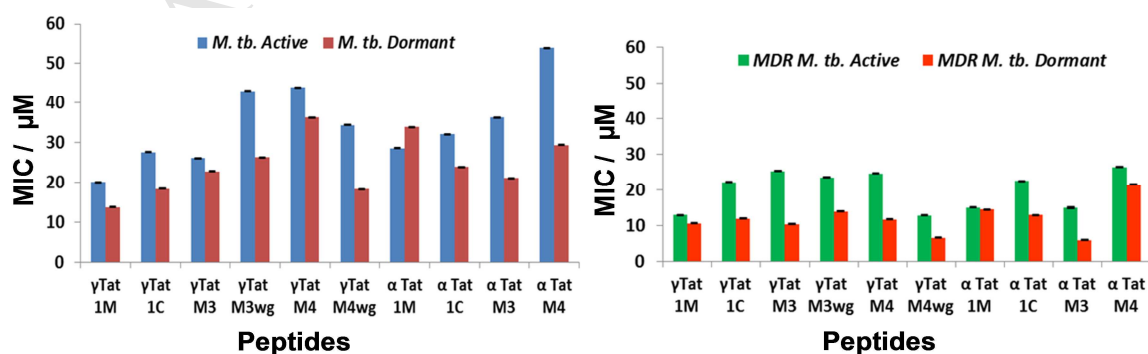


Figure 3. Activity of the peptides of the study against *Mycobacterium tuberculosis*.Table 3. MIC data (μM) for peptides of the study against *Mycobacterium tuberculosis in vitro*.

Peptide	MIC (μM) values of peptides with SD (\pm)			
	Mtb H37Ra (ATCC 25177)		MDR-Mtb	
	Dormant	Active	Dormant	Active
γTat1M	13.8 ± 0.001	20.1 ± 0.00076	10.6 ± 0.0015	13 ± 0.0035
γTat1C	18.4 ± 0.001	27.6 ± 0.00064	12.0 ± 0.001	22.1 ± 0.003
γTatM3	22.8 ± 0.003	26.1 ± 0.003	10.4 ± 0.0014	25.3 ± 0.0014
$\gamma\text{TatM3wg}$	26.3 ± 0.003	43.0 ± 0.0029	14.0 ± 0.001	23.5 ± 0.001
γTatM4	36.3 ± 0.003	43.9 ± 0.0026	11.7 ± 0.001	24.6 ± 0.0023
$\gamma\text{TatM4wg}$	18.3 ± 0.003	34.4 ± 0.003	6.6 ± 0.001	12.0 ± 0.002
αTat1M	33.9 ± 0.0042	28.6 ± 0.0042	14.5 ± 0.0026	15.1 ± 0.0026
αTat1C	23.9 ± 0.003	32.10 ± 0.003	12.9 ± 0.002	22.5 ± 0.0025
αTatM3	21.1 ± 0.0045	36.3 ± 0.0047	6.0 ± 0.0034	15.0 ± 0.0034
αTatM4	29.4 ± 0.004	53.9 ± 0.0036	21.5 ± 0.003	26.4 ± 0.0026
Rifampicin ^a	0.91 ± 0.005	0.97 ± 0.005	$>12.1 \pm 0.0037$	$>12.1 \pm 0.0043$
Pyrazinamide ^a	> 100	> 100	> 100	> 100

Anti-TB activity of each peptide was determined by serial dose dependent dilutions. Data are expressed as the mean values of triplicates. ^aStandard anti-TB drug and positive control.

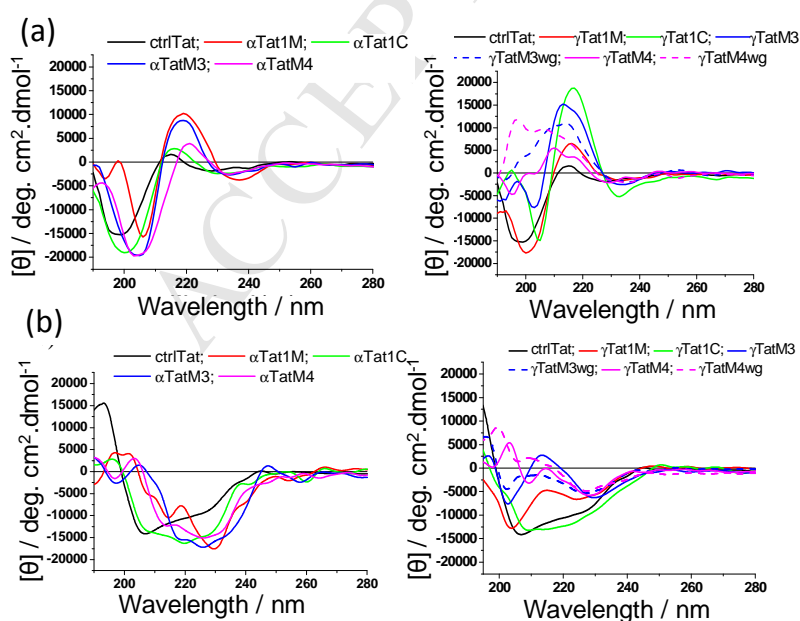


Figure 4. CD spectra of the all- α -Tat peptides and α,γ -Tat peptides of the study in water (a) and in 90% TFE-water (b).

Fluorescence- and transmission electron microscopy images

Fluorescence microscopy images were recorded using a dual staining method [LIVE/DEAD™ BacLight™ Bacterial Viability Kit, (Invitrogen)] employing SYTO 9 and propidium iodide (PI) dyes. As seen in Figure 5, significantly increased staining with PI is observed in cells treated with a representative peptide of the study in comparison to untreated cells.

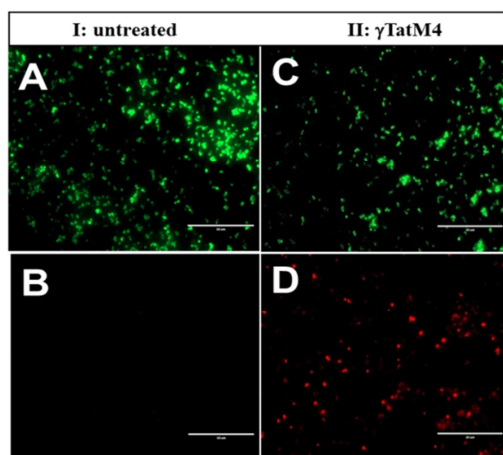


Figure 5. Fluorescence micrographs of *S. aureus*. A and C are green channel (SYTO 9)-; B and D are red channel (PI)- images captured for untreated cells (I) and cells treated with γ TatM4 (II) under 60X magnification respectively. Scale bar = 50 μ .

Representative Tat-peptides that displayed relatively higher antibacterial activity were studied by TEM to examine their effect on the bacterial cell walls. Specifically, the effect of the peptides γ TatM4 and γ Tat1C were studied on cells of *S. aureus* and *E. coli* as Gram-positive and Gram-negative bacteria respectively and are depicted in Figures 6 and 7 and on Mtb (Figure 8). Extensive damage to the bacterial membranes was observed.

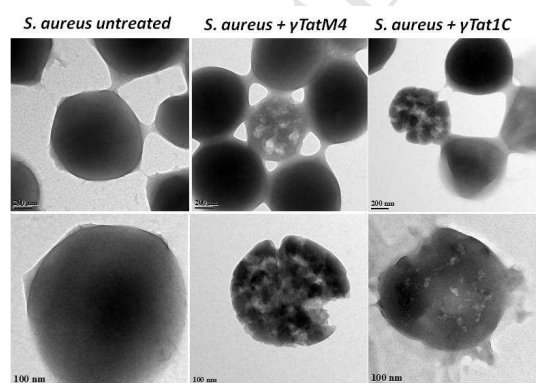


Figure 6. TEM images of *S. aureus* untreated and after treatment with representative peptides of the study. Scale bar: upper panel = 200 nm; lower panel = 100 nm.

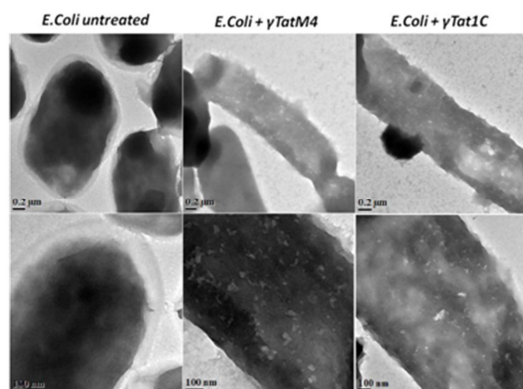


Figure 7. TEM images of *E. coli* untreated and after treatment with representative peptides of the study. Scale bar: upper panel = 200 nm; lower panel = 100 nm.

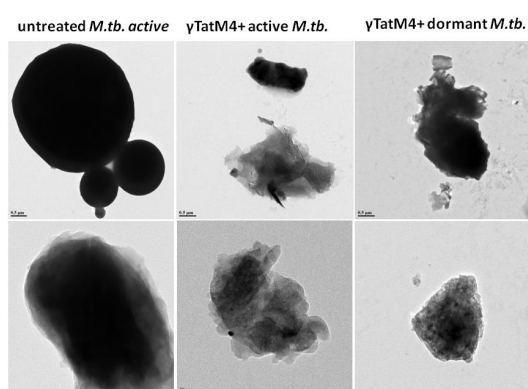


Figure 8. TEM images of *M. tuberculosis* untreated and after treatment with γ TatM4, a representative peptide of the study. Scale bar: upper panel = 0.5 μ ; lower panel = 50 nm.

Cytotoxicity studies

The cytotoxicity of the Tat peptides of the study on mammalian cells was estimated by the standard MTT cell viability assay. HeLa cells were treated with the peptides of the study at varying concentrations for 24 h and the cell viability was estimated. The results are depicted in Figure 9. As seen in the plot, the peptides of the study show very low cytotoxicity to mammalian cells. The cell viability is ≥ 80 % for almost all the peptides even at the higher concentrations studied. The cytotoxicity of the peptides was also evaluated in HCT 116 and HUVEC cells (SI).

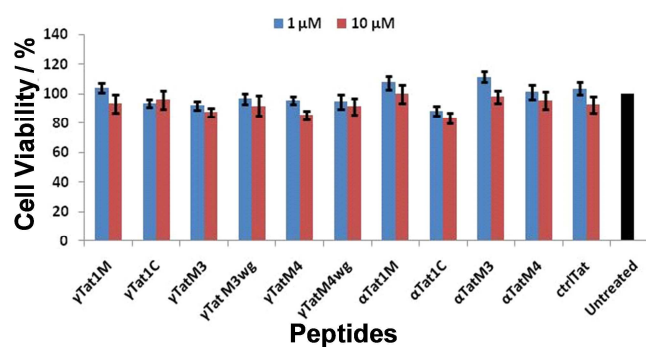


Figure 9. MTT cell viability assay upon treatment with Tat peptides of the study with HeLa cells.

The hemolytic activity of a representative Tat peptide analogue, γ TatM4, in comparison to the ctrlTat peptide, was measured as an indication of its effect on the mammalian cell membrane. This *in vitro* assay is an indicator of red blood cell lysis and evaluates the hemoglobin released in the plasma spectrophotometrically at 540 nm, after exposure to the test peptides. An increase in absorbance at this wavelength, is therefore, indicative of increased hemolysis and toxicity. The γ TatM4 peptide showed lower hemolytic activity compared to ctrlTat peptide (Figure 10). Treatment with Triton X-100 and phosphate buffered saline were used as positive and negative controls respectively. The results are in agreement with the cytotoxicity data obtained by the MTT assay (Figure 9).

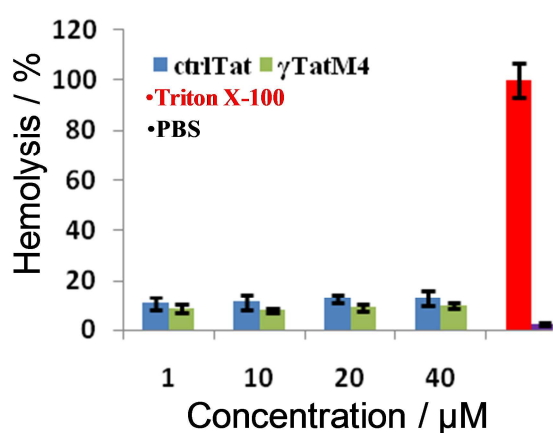


Figure 10. Hemolytic activity of representative peptides.

Stability to enzymatic hydrolysis

The stability of the Tat peptides of the study to hydrolytic digestion by enzymes was studied by treating the peptides with trypsin, a commercially available protease, and estimating the percent intact peptide remaining over time by HPLC analysis. The results of such a study with γ TatM4 as a representative example, in comparison to the control Tat peptide (ctrlTat) is shown in Figure 11. It is evident that the introduction of the arginine surrogate *r* within the Tat peptide sequence conferred the derived peptide with significant resistance to digestion by trypsin. In particular, the $t_{1/2}$ of γ TatM4 was found to be 16 h in comparison to 4 h for the ctrlTat peptide. After 24 h, 30% of the γ TatM4 peptide still remained intact, while only 4% of the ctrlTat peptide was found to be intact at the same time point. The fragments obtained after digestion with trypsin were analysed by MALDI-TOF. The results are tabulated in the SI. In the case of the ctrlTat peptide, cleavage was observed at the C-terminal sites of most of the lysine and arginine residues. Five fragments, in addition to the intact peptide were observed for the ctrlTat peptide even after 0.5 h, while the γ TatM4 peptide was completely intact at this time, with no observed fragmentation. The molecular ion of the intact γ TatM4 peptide was observed even after 24 h, and cleavage was observed to occur only at the C-termini of the K1 and R2 residues, while the other cleavage sites were blocked by the presence of the arginine analogues of the study. On the other hand, the molecular ion peak of the ctrlTat

peptide was completely absent after only 8 h. Exposure to the enzymes chymotrypsin and pepsin also confirmed the superior stability of γ TatM4 to proteolytic digestion in comparison to ctrlTat (SI).

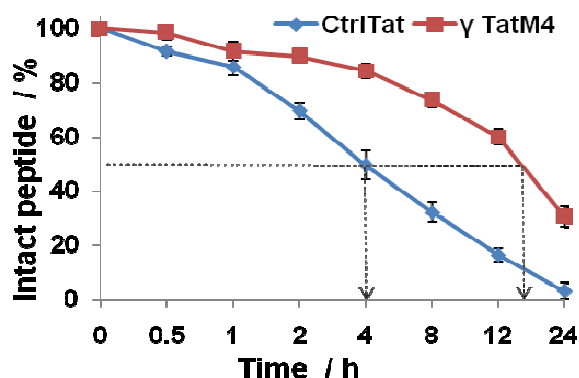


Figure 11. Stability of the γ TatM4 and ctrlTat peptides to proteolytic digestion by trypsin.

Discussion

Gram-positive and Gram-negative bacteria differ in the structure and composition of their cell walls, which could lead to differential interactions on their surface. However, both types of bacterial cell surfaces are negatively charged. The negative charge in Gram-positive bacteria is mainly due to the teichoic acid polymeric chains which bear anionic phosphates in the glycerolphosphate units, while in Gram-negative bacteria, this comes mainly from the phosphates and carboxylates of sugar acids. The overall negative charge makes them amenable to interaction with positively charged ligands, such as the Tat-peptides of the present study. The antibacterial effect of the α,γ -peptides of the study is far superior to that of the all- α -peptides. Among all the peptides, the γ TatM4 peptide displayed the best activity. The MIC values of the γ TatM4 peptide (0.61 to 1.35 μ M) are in the range or even better than those of some of the most effective antibiotics, e.g., ampicillin and kanamycin, currently used against the tested bacteria. This activity is also significantly more than reported for some natural antimicrobial peptides such as indolicidin, defensin, mellitin and magainin, against some of the tested bacteria.³⁸ The α,γ -peptides were also more active than the all- α -peptides against Mtb. It is indeed noteworthy that while the control Tat peptide showed insignificant activity against active and dormant forms of Mtb and MDR-Mtb (MIC > 150 μ M), all the peptides of the study were active to different extents. Although the MIC values for the Tat peptides of the study were not as low as for rifampicin against Mtb, it is noteworthy that many of the peptides are active against both, active and dormant forms of MDR-Mtb. It may be pointed out that most of the currently used drugs against Mtb, including rifampicin, act less effectively against the dormant forms. Importantly, the peptides reported herein act to a greater extent against MDR-Mtb than against Mtb itself. This is a particularly significant finding, since the treatment of MDR-Mtb is known to be increasingly challenging.

The observed antimicrobial properties of the Tat peptide analogues of this study could be a consequence of their increased amphipathic character, caused by the inclusion of the non-

natural amino acid surrogates. The increased hydrophobicity in comparison to ctrlTat could partly contribute to the cell membrane disruption and hence antimicrobial properties⁴² of the Tat peptide analogues described herein. The presence of the guanidine group rather than the amino group was also shown to be favourable for increased activity. The ability of the guanidine group to partake in bidentate hydrogen-bonding makes oligomers bearing this function more potent than those bearing simple amines. Thus, the peptide γ TatM4 was more active than the peptide γ TatM4wg. The highest activity was observed for the γ TatM4 peptide that bears four units of the γ -amino acid, r , while the peptides with fewer r units or bearing the α -amino acid, P^g , displayed lower antimicrobial activity. In general, the non-natural amino acid r , presenting the guanidino group on a relatively flexible alkyl spacer had a more positive effect on the antimicrobial properties of the resulting peptide, rather than the amino acid P^g , where the guanidino group is attached directly to the pyrrolidine ring in a more rigid disposition. The flexibility associated with the alkyl spacer could be the reason for more favourable interactions of the guanidines with the cell membrane in the derived α,γ -peptides, thus leading to their enhanced activity. The potent antimicrobial activity of Tat-derived AMPs indicated that they have potential to be used alone for the treatment of infections caused by both Gram-positive and Gram-negative bacteria. Although the use of a single agent to treat infections is the most commonly used practice, combination treatment can potentially eliminate drug resistant strains, delay the evolution of drug resistance and reduce the size of the dose, which can circumvent the side-effects.

The Tat₄₇₋₅₈ peptide is reported to display a CD signature commensurate with a random coil structure, even in the presence of TFE,^{36,20} while the longer Tat₄₇₋₇₂ peptide was reported to display a significant increase in the alpha-helical content in 80% TFE.³⁶ The ctrlTat peptide in our study displayed a random coil structure in water, as reported earlier,³⁶ but showed a significant change towards the α -helical structure in the presence of TFE. The CD studies suggest a possible correlation between the secondary structure of the peptides and their antimicrobial activity. Further, our studies indicate that the peptides that lack a defined secondary structure as seen for α -peptides, even in presence of the secondary structure-inducing solvent, trifluoroethanol (TFE), are more effective antibacterial agents in comparison to those that show a signature similar to that of an α -helix in the case of α -peptides, in presence of TFE. Thus, our findings suggest that though the structure of the Tat peptide analogues does seem to play a role in deciding their antibacterial activity, the helical component in the structure may not be as important as previously suggested in several literature reports.^{4,6-8} A helical predisposition may prove beneficial in terms of antimicrobial activity in the case of some peptides, but is not an absolute requirement, and potent activity may still be achieved with peptides that are not helically predisposed.

Of the two dyes used in the fluorescence microscopy studies, SYTO 9 can penetrate the cell membrane and bind strongly to DNA; it can be used to stain both live and dead cells. When bound to double-stranded DNA, its green fluorescence emission at 503 nm is enhanced (excitation maximum = 483 nm). PI, on the other hand, is membrane impermeant and is generally excluded from viable cells. It is therefore, commonly used to identify dead cells (where the cells are ruptured, with a release of the intracellular constituents into the

extracellular space) in a mixed population of dead and viable cells. When intercalated in nucleic acids, its emission maximum is at 617 nm (excitation at 535 nm). The relatively higher level of PI-staining in relation to SYTO 9-staining in the case of the γ TatM4 peptide analogue (Figure 5) is therefore, indicative of their higher ability to disrupt bacterial membranes in comparison to untreated. The TEM images (Figures 6 and 7) clearly illustrate the extensive damage that is caused to the bacterial cell walls, as previously suggested by studies with model membranes,²⁴ upon treatment with the Tat-peptides of the study. Further, the disruptive effects of the peptides are seen to affect both, Gram-positive as well as Gram-negative bacteria, with similar efficacy. The permeation of the cell wall can be seen in several cases in the form of pores or holes, causing the leakage of intracellular contents and leading to the formation of empty or dead cells. A similar devastating effect was observed with Mtb, when both active and dormant forms were significantly found to be affected (Figure 8), leading to permeation of the cell membranes and cell death.

The cytotoxicity of the Tat peptides of the study on mammalian cells (HeLa) was estimated by the MTT cell viability assay. It is a colorimetric assay that is based on the reduction of the tetrazolium dye, 3-(4,5-dimethylthiazol-2-yl)-2,5-diphenyltetrazolium bromide to a purple formazan derivative, that is achieved by enzymes present in viable cells. A decreased colour intensity is therefore indicative of low cell viability as a result of increased cytotoxicity. The peptides of the study showed low cytotoxic effects, with viability \geq 70-80 % at elevated concentrations (Figure 9). The low cytotoxic effect was also estimated and confirmed by the hemolysis assay, when the γ TatM4 peptide showed lower hemolytic activity than the ctrlTat peptide (Figure 10). The difference in deleterious effects observed with bacteria/ Mtb *vis-a-vis* mammalian cells could be attributed to the difference in composition of the bacterial and mammalian cell membranes, which may be expected to influence the interaction properties of the peptides with the respective membranes.

A major limitation of antimicrobial peptides is their inactivation by proteases. Poor protease stability severely limits the clinical use of potentially therapeutic peptides. The Tat-peptide contains multiple arginine and lysine residues, which constitute the proteolytic sites (at their C-termini) of the enzyme trypsin,⁴⁰ thus making it an ideal enzyme for a study of their protease resistance. The non-natural amino acids used in the present work confer the derived peptide with improved protease resistance properties, increasing their application potential in biological systems, by increasing their half-life significantly. MALDI-TOF analysis of the fragments obtained after trypsin digestion reaffirmed the protective effect the amino acid surrogates.

Conclusions

The Tat peptide has been reported to have some antifungal activity against human pathogenic fungi,²⁸ but so far, there are only few reports concerning its antibacterial effects and no reports of its anti-TB effects, this being the first. Further, in contrast to the antifungal effect, where no disruption of fungal membranes was observed, and the antifungal effect was found to be due to the arrest of the G1 phase of the fungal cell cycle after penetration into the

nucleus,²⁸ the antibacterial and anti-TB effects were found to be due to the interaction with and disruption of microbial membranes, leading to cell lysis and death, as earlier reported.^{23,24} Both electrostatic as well as hydrophobic interactions are possibly involved in bringing about this effect. The detailed mechanism of action against Mtb is not known as yet. From our TEM results, the anti-TB effect appears to be by membrane disruption, as with Gram-positive and Gram-negative bacteria. The applicability of the peptides reported herein could be enhanced, perhaps synergistically, by combination with known antimicrobial agents such as antibiotics.⁴¹ This possibility is actively being pursued in our laboratory.

On the whole, the Tat peptide analogues reported herein are shown to possess good activity against Gram-positive and Gram-negative bacteria and also Mtb. The fact that they are active particularly against the dormant forms of Mtb, in addition to the active form, makes them promising for further study and development. Their low potential for resistance development combined with their higher bio-stability, owing to the presence of non-natural amino acids, further adds to their potential towards therapy.

Experimental Section

General Information

All the reagents used were obtained commercially and were of $\geq 95\%$ purity and used without further purification. DMF, CH_2Cl_2 , pyridine were dried over P_2O_5 , CaH_2 , KOH respectively. DMF, CH_2Cl_2 were stored by adding 4 Å molecular sieves and pyridine by adding KOH. Column chromatography was performed for purification of compounds on silica gel (100-200 mesh or 60-120 mesh, Merck). TLCs were performed on pre-coated with silica gel 60 F254 (Merck) aluminium sheets. TLCs were performed using petroleum ether-ethyl acetate and ethyl acetate-methanol solvent systems. TLCs were visualised after spraying with ninhydrin reagent and heating. ^1H and ^{13}C NMR spectra were recorded on a Bruker AV 200 or AV 400 or AV 500 spectrometer fitted with an Aspect 3000 computer and all the chemical shifts (ppm) are referred to internal TMS, chloroform-*d* for ^1H and/or ^{13}C NMR. ^1H NMR data are reported in the order of chemical shift, multiplicity (s, singlet; d, doublet; t, triplet; q, quartet; br, broad; br s, broad singlet; m, multiplet and/ or multiple resonance), number of protons. HRMS mass spectra were recorded on a Thermo Scientific Q-Exactive, Accela 1250 pump MALDI-TOF spectra were obtained from a Voyager-De-STR (Applied Biosystems) and CHCA (α -Cyano-4-hydroxycinnamic acid) matrix was used to analyze MALDI-TOF samples. All final compounds and oligomers were $\geq 95\%$ pure, as determined by ^1H NMR, ^{13}C NMR, HRMS, HPLC and/or MALDI-TOF analysis, as applicable. UV absorbance was performed on a Varian Cary 300 UV-VIS spectrophotometer.

Experimental procedures and spectral data

(2*S*,4*R*)-methyl-1-(3-(*tert*-butyloxycarbonyl-amino)propyl)-4-hydroxypyrrolidine-2-carboxylate (2)

To a 250 mL round bottom flask containing *trans*-4-hydroxy-L-proline methyl ester **1** (5 g, 34.5 mmol) dissolved in dry DMF (15 mL), triethylamine (14.4 mL, 103.0 mmol) and

catalytic amount of DMAP were added. The above reaction mixture was stirred for 30 min at room temperature and 2-((Boc)amino)propyl methanesulfonate (13.1 g, 51.5 mmol) dissolved in dry DMF was added drop-wise. The reaction was heated at 70 °C for 10 h and monitored by TLC. The solvent was evaporated *in vacuo* and the crude reaction mixture was taken up in ethyl acetate and water. The layers were separated, and the aqueous phase extracted with ethyl acetate. The combined organic extracts were washed with brine, dried over Na₂SO₄ and evaporated under vacuum. The crude product was purified by silica gel column chromatography using a gradient of ethyl acetate in petroleum ether to give title compound **2** as a pale yellow gummy liquid (6.4 g, 62%). [α]_D²⁰ -143.72 (*c* 0.1, CHCl₃). ¹H NMR (200 MHz, CDCl₃) δ : 5.38 (br s, 1H), 4.45 (m, 1H), 3.72 (s, 3H), 3.54 (m, 1H), 3.36 (m, 1H), 3.19 (m, 2H), 2.73 (m, 2H), 2.56 (m, 2H), 2.14 (m, 2H), 1.63 (m, 2H), 1.44 (s, 9H). ¹³C NMR (50 MHz, CDCl₃) δ : 174.4, 156.3, 77.1, 70.0, 64.4, 60.9, 51.8, 39.3, 38.5, 28.4, 28.0. ¹³C DEPT (50 MHz, CDCl₃) δ : 70.0, 64.4, 60.9, 51.9, 51.8, 39.3, 38.5, 28.4, 28.0. HRMS (ESI): *m/z* calculated for C₁₄H₂₆N₂O₅: 302.1842, Observed [M⁺+H]: 303.1915, [M⁺+Na]: 325.1713.

(2S,4S)-methyl-4-azido-1-(3-(tert-butyloxycarbonyl amino)propyl)pyrrolidine-2-carboxylate (3)

Dry triethylamine (10 mL) was added to a solution of compound **2** (5 g, 16.5 mmol) in dry CH₂Cl₂. The reaction mixture was stirred for 30 min, mesyl chloride (3.8 mL, 49.6 mmol) was added drop-wise by syringe and stirring continued for another 30 min at 0-5 °C. The reaction was monitored by TLC. Upon completion, excess of CH₂Cl₂ and water (100 mL) were added. The layers were separated, and the aqueous phase was extracted with CH₂Cl₂ (3 x 100 mL). The combined organic extracts were washed with brine (100 mL), dried over Na₂SO₄. The solvents were evaporated *in vacuo* and the mesylate obtained was used in the further reaction. The mesyl compound was dissolved in dry DMF (10 mL) and sodium azide (2.56 g, 39.5 mmol) was added portion-wise at room temperature with constant stirring. The reaction was heated at 65 °C for the next 6 h and monitored by TLC. Upon completion of reaction, solvent was evaporated *in vacuo*, followed by addition of ethyl acetate and water. The layers were separated, and the aqueous phase was extracted with ethyl acetate. The combined organic extracts were washed with brine, dried over Na₂SO₄ and evaporated. The crude residue was purified by silica gel column chromatography using a gradient of ethyl acetate in petroleum ether to give the title compound **3** as a pale yellow solid (1.72 g, 67%). [α]_D²⁰ -137.92 (*c* 0.1, CHCl₃). ¹H NMR (200 MHz, CDCl₃) δ : 5.47 (br s, 1H, NH), 3.96 (m, 1H), 3.77 (s, 3H), 3.25 (m, 4H), 2.88 (m, 1H), 2.53 (m, 3H), 2.15 (m, 1H), 1.44 (s, 9H). ¹³C NMR (50 MHz, CDCl₃) δ : 173.3, 156.2, 78.6, 64.8, 58.7, 58.0, 52.1, 51.7, 38.5, 35.4, 28.4, 27.8. ¹³C DEPT (50 MHz, CDCl₃) δ : 64.8, 58.7, 58.0, 52.1, 51.7, 38.4, 35.4, 28.4, 27.7. HRMS (ESI): *m/z* calculated for C₁₄H₂₅N₅O₄: 327.1907; observed [M⁺+H]: 328.1977; [M⁺+Na]: 342.2131.

(2S,4R)-4-(((9H-fluoren-9 yl)methoxy)carbonyl)amino)-1-(3-(tert-butyloxycarbonyl amino)propyl)pyrrolidine-2-carboxylic acid (X)

To a solution of azido compound **3** (1.5 g, 4.58 mmol) dissolved in dry MeOH (25 mL), 10% palladium on charcoal (300 mg, 20% w/w) was added and the resulting reaction mixture stirred under hydrogen gas at 50 psi for 3 h and the reaction was monitored by TLC. After

completion of reaction, it was filtered through celite and water:methanol (1:1, 10 mL) were added. 2N LiOH (15 mL) was further added and the reaction was stirred for 30 min. Methanol was evaporated under reduced pressure and the resulting reaction mixture was neutralised with dil. HCl. The solvents were evaporated and the residue was suspended in methanol and filtered. The supernatant was evaporated *in vacuo* and dried in a desiccator to give the corresponding amino acid. To a solution of the amino acid, dissolved in 1, 4-dioxane:water (1:1, 5 ml), NaHCO₃ (3.0 g, 36 mmol) was added to maintain an alkaline pH. The resulting reaction mixture was stirred at room temperature for 30 min and Fmoc-Cl (2.69 g, 10.4 mmol) was added slowly. Stirring was further continued overnight at room temperature. The reaction was monitored by TLC. Upon completion of reaction, the reaction mixture was made slightly acidic by addition of Dowex H⁺ resin, which was subsequently filtered off. The dioxane was removed under vacuum and the crude compound extracted in ethyl acetate. The combined organic extracts were washed with brine and dried over sodium sulfate and evaporated *in vacuo*. The crude product was purified by silica gel column chromatography to give the title compound **X** (1.02 gm, 58 %) as a solid yellowish foam. $[\alpha]_D^{20}$ -27.36 (*c* 0.1, CHCl₃). ¹H NMR (200 MHz, CDCl₃) δ : 7.75 (m, 2H), 7.57 (m, 2H), 7.34 (m, 4H), 4.61 (m, 1H), 4.38 (m, 2H), 4.21 (m, 2H), 3.77 (m, 1H), 3.13 (m, 3H), 2.80 (m, 1H), 2.53 (m, 2H), 2.33 (m, 1H), 2.00 (m, 2H), 1.46 & 1.44 (s, 9H). ¹³C NMR (50 MHz, CDCl₃) δ : 174.3, 155.9, 144.0, 141.3, 127.1, 120.0, 79.0, 66.6, 64.4, 52.2, 47.3, 36.8, 28.1. ¹³C DEPT (50 MHz, CDCl₃) δ : 127.0, 124.7, 119.9, 66.6, 64.4, 52.2, 47.2, 36.8, 28.4. HRMS (ESI): *m/z* calculated for C₂₈H₃₅N₃O₆: 509.2526; observed: [M⁺+H] 510.2596, [M⁺+Na] 532.2411.

(2S,4R)-methyl-1-(tert-butyloxycarbonyl)-4-hydroxypyrrolidine-2-carboxylate (4)

To a solution of *trans*-4-hydroxy-L-proline methyl ester **1** (10 g, 68.9 mmol) dissolved in dioxane:water (1:1, 25 ml), sodium hydroxide (8.26 g, 206.7 mmol) was added. The reaction mixture was stirred for 30 min at room temperature, followed by drop-wise addition of di-*tert*-butyl dicarbonate (19.54 g, 89.5 mmol) dissolved in dioxane:water (1:1). The reaction was further stirred at RT for 4 h and monitored by TLC. Upon completion of reaction, the dioxane was removed under vacuum and ethyl acetate was added. The layers were separated, and the aqueous phase was extracted with ethyl acetate. The combined organic extracts were washed with brine and dried over Na₂SO₄. The solvent was evaporated and the crude residue was purified by silica gel column chromatography to give the title compound **4** as a white crystalline solid (14.2 g, 84%). $[\alpha]_D^{20}$ = -134.30 (*c* 0.080, CHCl₃). ¹H NMR (200 MHz, CDCl₃) δ : 4.43 (m,1H), 4.36 (m,1H), 3.70 (s,3H), 3.56 (d, *J* = 3.4 Hz,1H), 3.52 (d, *J* = 11.6 Hz,1H), 2.25 (m, 1H), 2.01 (m,1H), 1.42 (s, major) & 1.37 (s, minor), 9H. ¹³C NMR (50 MHz, CDCl₃) δ : 173.7, 154.0, 80.4, 69.1, 57.9, 54.6, 52.0, 39.0, 28.2. ¹³C DEPT (50 MHz, CDCl₃) δ : 69.1, 57.9, 54.6, 52.0, 39.0, 28.2. HRMS (ESI): *m/z* calculated for C₁₁H₁₉NO₅: 245.1263; Observed: [M⁺+Na] 268.1151.

(2S,4S)-methyl-1-(tert-butyloxycarbonyl)-4-azidopyrrolidine-2-carboxylate (5)

Dry triethylamine (6 mL) was added to a solution of compound **4** (3.0 g, 12.2 mmol) in dry CH₂Cl₂. The reaction mixture was stirred for 30 min and mesyl chloride (1.42 mL, 18.4 mmol) was added drop-wise and stirring continued for another 30 min at 0-5 °C. The reaction

was monitored by TLC. Upon completion of reaction, excess CH_2Cl_2 and water (100 mL) were added. The layers were separated, and the aqueous phase was extracted with CH_2Cl_2 (3 x 100 mL). The combined organic extracts were washed with brine (100 mL), dried over Na_2SO_4 . The solvents were evaporated *in vacuo* and the mesylate obtained was used in the further reaction. To a flask containing the mesyl compound dissolved in dry DMF, was added sodium azide (2 g, 6.19 mmol) portion-wise at room temperature with constant stirring. The reaction was heated at 65 °C for 10 h, and monitored by TLC. Upon completion of reaction, the solvent was evaporated *in vacuo* and ethyl acetate and water were added to the residue. The layers were separated, and the aqueous phase was further extracted with ethyl acetate. The combined organic extracts were washed with brine and dried over Na_2SO_4 . The solvent was evaporated under vacuum and the crude product was purified by silica gel column chromatography to give the title compound **5** as a thick gummy liquid (1.12 g, 67%). $[\alpha]_{\text{D}}^{20}$ -71.13 (*c* 0.065, CHCl_3). ^1H NMR (200 MHz, CDCl_3) δ : 4.41 (min) & 4.31 (maj) (m, 1H), 4.15 (m, 1H), 3.73 (s, 3H), 3.66 (d, *J* = 4.0 Hz, 1H), 3.46 (d, *J* = 4.0 Hz, 1H), 2.44 (m, 1H), 2.16 (dd, *J* = 1.0 & 4.0 Hz, 1H), 1.45 (min) & 1.39 (maj) (s, 9H). ^{13}C NMR (50 MHz, CDCl_3) δ : 172.2, 153.0, 80.5, 59.2, 52.2, 51.2, 35.0, 28.1. ^{13}C DEPT (50 MHz, CDCl_3) δ : 59.2, 57.6, 52.2, 51.2, 35.9, 28.1. HRMS (ESI): *m/z* calculated for $\text{C}_{11}\text{H}_{18}\text{N}_4\text{O}_4$: 270.1328; Observed: $[\text{M}^+ + \text{Na}]$ 293.1214.

(2*S*,4*S*)-4-((((9*H*-fluoren-9-yl)methoxy)carbonyl)amino)-1-(*tert*-butoxycarbonyl)pyrrolidine-2-carboxylic acid (Z**)**

To a solution of azido compound **5** (1.5 g, 5.5 mmol) dissolved in dry MeOH (25 mL), 10% palladium on charcoal (300 mg, 20% w/w) was added, the resulting reaction mixture stirred under hydrogen gas at 50 psi for 3 h and the reaction was monitored by TLC. After completion of reaction, it was filtered through celite and water and methanol (1:1, 10 mL) were added. 2 N LiOH (15 mL) was further added to the reaction mixture and stirred for 30 min. Methanol was evaporated under reduced pressure and the resulting mixture was neutralised with dil. HCl. Solvents were evaporated and the residue was suspended in methanol and filtered. The supernatant collected was evaporated *in vacuo* to obtain the corresponding amino acid. The amino acid obtained was dissolved in 1, 4-dioxane:water (1:1), and NaHCO_3 (3.6 g, 43.4 mmol) was added to ensure an alkaline pH. The resulting reaction mixture was stirred at room temperature for 30 min and Fmoc-Cl (1.33 g, 5.1 mmol) was added in portions. The reaction mixture was stirred overnight at room temperature and monitored by TLC. Upon completion of reaction, the reaction mixture was slightly acidified by addition of Dowex H^+ resin and the resin was subsequently filtered off. The dioxane was evaporated under vacuum and ethyl acetate was added. The product was extracted in ethyl acetate. The organic extracts were washed with brine and dried over sodium sulfate. The solvents were evaporated *in vacuo* and the product was washed repeatedly by petroleum ether and diethyl ether to give title compound **Z** (1.13 g, 58%) as a solid yellowish foam. $[\alpha]_{\text{D}}^{20}$ -69.60 (*c* 0.050, CHCl_3). ^1H NMR (200 MHz, CDCl_3) δ : 7.74 (m, 2H), 7.57 (m, 2H), 7.40 (m, 4H), 5.80 (m, 1H), 4.49 (m, 2H), 4.34 (m, 3H), 4.20 (m, 1H), 3.53 (m, 2H), 2.38 (m, 1H), 1.50 & 1.44 (s, 9H). ^{13}C NMR (50 MHz, CDCl_3) δ : 174.5, 156.7, 156.0, 143.8, 142.6, 141.3, 127.8, 120.0, 82.4, 67.1, 58.4, 47.1, 28.3. ^{13}C DEPT (50 MHz, CDCl_3) δ : 125.8, 125.2,

122.3, 118.1, 65.2, 56.5, 51.8, 45.2, 31.7, 26.4. HRMS (ESI): m/z calculated for $C_{25}H_{28}N_2O_6$: 452.1947; Observed: $[M^+ + Na]$ 475.1832.

Solid phase peptide synthesis of Tat analogues

All the peptides were synthesized using standard Boc- or Fmoc- chemistry protocol and MBHA (4-methyl-benzhydrylamine) resin as the solid support (SI). Synthesis was carried out on 50 μ mol scale manually. Removal of the Fmoc-or Boc-group was carried out using 20% piperidine in DMF or 50% TFA in CH_2Cl_2 respectively. Boc-removal was followed by neutralization using 5% DIPEA in DCM. Further coupling reactions were performed by use of three equivalents each of monomeric amino acid, TBTU, HOBt and DIPEA in DMF for 6 h. Successive deprotection, coupling and washing steps were carried out as iterative cycles until the desired length of peptide was synthesized. The *N*-terminal Fmoc- or Boc-protecting groups in the completely synthesized peptides were finally cleaved using piperidine/ DMF or TFA/ CH_2Cl_2 respectively as described above, and the resulting amines capped as acetates using acetic anhydride in 50% pyridine/ DCM. All the deprotection and coupling reactions were monitored by the Kaiser test. Guanidinylation of pendant amines on solid phase was performed by using 10 equivalents of 1-*H*-pyrazole-1-carboxamide hydrochloride reagent and 10 equivalents (corresponding to each amino group) DIPEA in DMF overnight.

Cleavage and purification of resin bound peptide

After synthesis of the desired peptide sequences, they were cleaved from the solid support by TFA-TFMSA cleavage protocol. In detail, 5 mg of dry peptide-bound resin was taken in a glass sample vial. Thioanisole (10 μ L) and 1, 2-dithian (4 μ L) were added to it. After 5 min, to the ice-cooled sample vial, 80 μ L of TFA was added. After another 10 min, 8 μ L of TFMSA was added with slow shaking and the resultant reaction mixture was kept for the next 2 h to ensure removal of all the side chain protecting groups and complete detachment of the peptide from the resin support. After 2 h, the residual resin was filtered off through a sintered funnel and washed with neat TFA. The filtrate was evaporated on a rotary evaporator and cold diethylether was added. The resulting precipitate was then separated by centrifugation and water was added. This crude peptide was further purified by RP-HPLC on a C-18 column using an increasing gradient of acetonitrile in water containing 0.1 % TFA. The peptides were re-confirmed to be ≥ 95 % pure by analytical HPLC and MALDI-TOF analysis.

Anti-bacterial activity

All bacterial cultures were first grown in LB media at 37 $^\circ$ C at 180 rpm. Once the culture reached an absorbance of 1 OD, as measured at 620 nm, it was used for anti-bacterial assays. Bacterial strains *E. coli* (NCIM 2688), *P. aeruginosa* (NCIM 2036), *Enterobacter spp.* (NCIM 5392) as Gram-negative and *B. subtilis* (NCIM 2079), *S. aureus* (NCIM 2010), *S. epidermidis* (NCIM 5270) as Gram-positive were obtained from NCIM (CSIR-NCL, Pune) and were grown in Luria Bertani medium (Himedia, India). 0.1 % of 1 OD culture at 600 nm was used for screening. 0.1 % inoculated culture was added into each well of the 96-well plate containing the compounds to be tested. Optical density for each plate was measured at 620 nm after 8 h for Gram-negative bacteria and after 12 h for Gram-positive bacteria.

Anti-TB assay

All the synthetic peptides were screened for their *in vitro* activity against *M. tuberculosis* H37Ra (Mtb) (ATCC 25177) and multidrug resistant *M. tuberculosis* H37Ra (MDR-Mtb). MICs were determined in both these strains by using the standard XTT Reduction Menadione Assay (XRMA) protocol previously described by Singh *et al.*⁴² Briefly, 2.5 μ l aliquots of 2-fold serially diluted peptides were mixed in 247.5 μ l of *Mtb*/MDR *Mtb* inoculated cultures ($\sim 5 \times 10^5$ cells/ml) in 96-well plates and sealed with plate sealer (Nunc Inc.). After incubation at 37 °C, the XTT menadione assay was performed after 8 days for detection of active stage inhibitors and 12 days for detection of dormant stage inhibitors respectively, by removing the plate sealer. Absorbance was measured at 470 nm and percentage inhibition was calculated using the formula: % inhibition = [(Control – Test) / (Control – Blank)] x 100, where ‘Control’ is the absorbance in the absence of added compounds, ‘Test’ is the absorbance in the presence of compounds and ‘Blank’ is the absorbance of the culture medium without mycobacteria.

CD analysis

The secondary structures of the peptides in different environments were measured using a J-815 spectropolarimeter (Jasco, Japan). The spectra were recorded at a scan speed of 100 nm/min at wavelengths ranging from 190 to 300 nm in water and 90 % TFE (Sigma). An average of three scans was collected for each peptide. The final concentration of the peptides was 500 μ M. The acquired CD signal spectra were converted to the molar ellipticity using the equation: $[\theta] = (\theta \times 1000) / (c \times l)$, where, $[\theta]$ is the molar ellipticity ($\text{deg} \cdot \text{cm}^2 \cdot \text{dmol}^{-1}$), θ is the observed ellipticity corrected for the buffer at a given wavelength (mdeg), c is the peptide concentration (M), l is the path length (cm).

Fluorescence microscopy images

S. aureus was allowed to grow to the mid-log phase and then incubated with the peptides (10 μ g/mL) at 37 °C for 4 h. The solution was centrifuged at 1000 g for 10 min. The supernatant was removed and the bacterial pellets were washed with PBS three to four times. PI (5 μ g/mL) was added and incubated for 15 min in the dark. Excess dye was removed by PBS washes ($\times 3$). Next, the cells were incubated with SYTO 9 (10 μ g/mL in water) for 15 min in the dark and excess dye was removed, followed by PBS washes ($\times 3$). The bacteria were then examined under oil-immersion objective (60 X) by using the Invitrogen™ EVOS™ FL Cell Imaging Microscope.

Transmission Electron Microscopy images

E. coli and *S. aureus* were cultured to mid-log phase. The cells were harvested by centrifugation at $1,000 \times g$ for 10 min, washed thrice with 10 mM PBS and re-suspended to an $\text{OD}_{600\text{nm}}$ of 0.2. The cell suspension was incubated at 37 °C for 60 min with different peptides at their MIC. Following the incubation, the cells were centrifuged and washed with PBS 3 times at 5,000 g for 5 min. Microbial cell pellets were then fixed overnight with 2.5 % (v/v) glutaraldehyde in PBS at 4 °C and washed twice with PBS. After pre-fixation with 2.5

% glutaraldehyde overnight, the cell pellets were washed 3 times with PBS and post-fixed with 2 % osmium tetroxide in PBS for 70 min. The samples were washed twice with PBS, followed by dehydration for 9 min in a graded ethanol series (50%, 70%, 90% and 100%), and incubated for 10 min each in 100% ethanol, a mixture (1:1) of 100% ethanol and acetone, and absolute acetone. These samples were then transferred to a constant-temperature (37 °C) incubator overnight. Finally, the specimens were observed using a transmission electron microscope.

Cytotoxicity studies: MTT cell viability and hemolysis assays

The cytotoxicity of peptides against cells was determined by the MTT cell viability assay. All cells were plated overnight in 96-well plates at a density of 10000 cells per well in 0.2 ml of appropriate growth medium with 10 % FBS at 37 °C. Different concentrations of peptides up to a maximum of 50 µM were incubated with the cell for 24 h, following which, the peptides were removed from the media by replacing with fresh media. Cell culture medium alone or with cells, both without peptides, were included in each experiment as controls. After 24 h incubation, 10 µL of 5 mg/ml of 3-(4,5-dimethylthiazol-2-yl)-2,5-diphenyl-tetrazolium bromide (MTT) was added and incubated for 4 h. Conversion of MTT into purple formazan product by metabolically active cells indicates the extent of cell viability. The crystals of formazan were dissolved with isopropanol and the optical density was measured at 570 nm using a Spectramax^{pro5} plate reader (Molecular Devices Inc) for quantification of cell viability.

In the hemolysis assay, freshly drawn human red blood cells (hRBCs) with additive K2 EDTA (spray-dried) were washed with PBS buffer several times and centrifuged at 1000 g for 10 min until a clear supernatant was observed. The hRBCs were re-suspended in 1× PBS to get a 0.5 % v/v suspension. Peptides dissolved in 1× PBS were added to a sterile 96-well plate to make up to a total volume of 75 µL in each well. Then 75 µL of 0.5 % v/v hRBC solution was added to make up a total volume of 150 µL in each well. The 0 % and 100 % hemolysis points were determined in 1 × PBS and 0.2 % Triton-X-100 respectively. The plate was then incubated at 37 °C for 1h, followed by centrifugation at 3500 rpm for 10 min. The supernatant (120 µL) was transferred to fresh wells and absorption was detected by measuring the (optical density at 414 nm by VarioskanFlash (4.00.53) Microplate Reader. Results were with respect to the positive Triton X-100) and negative (PBS) controls. % hemolysis was determined by the equation: % hemolysis = $(\text{Abs}_{\text{sample}} - \text{Abs}_{\text{PBS}}) / (\text{Abs}_{\text{Triton}} - \text{Abs}_{\text{PBS}}) \times 100$.

Trypsin Digestion Assay

A reverse phase high-performance liquid chromatography (RP-HPLC) assay was used to assess proteolytic susceptibility. Peptide concentration was calculated by measuring the absorbance at 260 nm and using the extinction co-efficient $\epsilon_{260\text{nm}} = 200 \text{ M}^{-1}\text{cm}^{-1}$ for phenylalanine. Peptide stock solutions were prepared in Tris-EDTA buffer. Cell culture grade trypsin from bovine pancreas was purchased from Thermo Fisher Scientific. Each trypsinolysis experiment was carried out at a peptide concentration of 10 mM, and run in triplicate. Following addition of trypsin (1 µL of 1X Tryple Express enzyme in 100 µL

peptide solution), aliquots of the reaction were removed at different time intervals and quenched by combining a 10 μ L aliquot of the trypsinolysis mixture with 10 μ L of 2 % trifluoroacetic acid in acetonitrile. A portion (20 μ L) of the quenched reaction mixture was subjected to RP-HPLC and the peaks obtained were analyzed. The extent of peptide trypsinolysis was determined by integrating the area of the peak corresponding to the intact peptide. The peaks observed in the HPLCs were collected and analyzed by matrix-assisted laser desorption/ionization–time of flight (MALDI-TOF) to identify the peptide fragments.

Acknowledgements

The Council of Scientific and Industrial Research, New Delhi, is gratefully acknowledged for a research grant (BSC0302). GSB thanks UGC, New Delhi, for a research fellowship.

References

- [1] a) I. M. Herzog, M. Fridman, *Med. Chem. Commun.*, **2014**, 5, 1014-1026. (b) M. N. Melo, R. Ferre, M. A. R. B. Castanho, *Nat. Rev. Microbiol.*, **2009**, 7, 245– 250.
- [2] (a) A. Sharma, A. A. Pohane, S. Bansal, A. Bajaj, V. Jain, A. Srivastava, *Chem. Eur. J.*, **2015**, 21, 3540-3545. (b) J. K. Lee, S. C. Park, K. S. Hahm, Y. Park, *Biomaterials*, **2014**, 35, 1025-1039. (c) S. B. Winfred, G. Meiyazagan, J. J. Panda, V. Nagendrababu, K. Deivanayagam, V. S. Chauhan, Venkatraman, *Eur. J. Dent.*, **2014**, 8, 254-260 (d) K. Lim, R. R. Y. Chua, R. Saravanan, A. Basu, B. Mishra, P. A. Tambyah, B. Ho, S. S. Leong, *ACS Appl. Mater. Interfaces*, **2013**, 5, 6412–6422. (e) R. P. Hicks, J. J. Abercrombie, R. K. Wong, K. P. Leung, *Bioorg. Med. Chem.*, **2013**, 21, 205–214. (f) A. A. Romani, M. C. Baroni, S. Taddei, F. Ghidini, P. Sansoni, S. Caviranib, C. S. Cabassib, *J. Pept. Sci.*, **2013**, 19, 554–565. (g) N. Stempel, J. Strehmel, J. Overhage, *Curr. Pharm. Des.*, **2015**, 21, 67-84. (h) J. Pinto da Costa, M. Cova, R. Ferreira, R. Vitorino, *Appl. Microbiol. Biotechnol.*, **2015**, 99, 2023–2040.
- [3] J. A. Patch, A. E. Barron, *Curr. Opin. Chem. Biol.*, **2002**, 6, 872–877.
- [4] M. Nepal, S. Thangamani, M. N. Seleem, J. Chmielewski, *Org. Biomol. Chem.*, **2015**, 13, 5930-5936.
- [5] R. Domalaon, X. Yang, J. O'Neil, G. G. Zhanel, N. Mookherjee, F. Schweizer, *Amino Acids*, **2014**, 46, 2517-2530.
- [6] K. Gademann, T. Hintermann, J. V. Schreiber, *Curr. Med. Chem.*, **1999**, 6, 905-925.
- [7] R. P. Cheng, S. H. Gellman, W. F. DeGrado, *Chem. Rev.*, **2001**, 101, 3219-3232.
- [8] E. A. Porter, B. Weisblum, S. H. Gellman, *J. Am. Chem. Soc.*, **2002**, 124, 7324-7330.
- [9] R. J. Simon, R. S. Kania, R. N. Zuckermann, V. D. Huebner, D. A. Jewell, S. Banville, S. Ng, L. Wang, S. Rosenberg, C. K. Marlowe, *Proc. Natl. Acad. Sci. U. S. A.*, **1992**, 89, 9367–9371.
- [10] X. Li, Y. D. Wu, D. Yang, *Acc. Chem. Res.*, **2008**, 41, 1428–1438.
- [11] W. S. Horne, L. M. Johnson, T. J. Ketas, P. J. Klasse, M. Lu, J. P. Moore, S. H. Gellman, *Proc. Natl. Acad. Sci. U. S. A.*, **2009**, 106, 14751–14756.
- [12] W. S. Horne, S. H. Gellman, *Acc. Chem. Res.*, **2008**, 41, 1399–1408.
- [13] H. J. Lee, J. W. Song, Y. S. Choi, H. M. Park, K. B. Lee, *J. Am. Chem. Soc.*, **2002**, 124, 11881–11893.
- [14] T. L. Graybill, M. J. Ross, B. R. Gauvin, B. S. Gregory, A. L. Harris, M. A. Ator, J. M. Rinker, R. E. Dolle, *Bioorg. Med. Chem. Lett.*, **1992**, 2, 1375–1380.
- [15] K. M. Wagstaff, D. A. Jans, *Curr. Med. Chem.*, **2006**, 13, 1371-1387.
- [16] (a) J. S. Wadia, R. V. Stan, S. F. Dowdy, *Nat. Med.* **2004**, 10, 310-315. (b) S. Kameyama, M. Horie, T. Kikuchi, T. Omura, T. Takeuchi, I. Nakase, Y. Sugiura, S. Futaki, *Bioconjugate Chem.*, **2006**, 17, 597–602.
- [17] (a) Y. L. Chiu, A. Ali, C. Y. Chu, H. Cao, T. M. Rana, *Chem. Biol.*, **2004**, 11, 1165-1175. (b) S. Tripathi, B. Chaubey, B. E. Barton, V. N. Pandey, *Virology*, **2007**, 363, 91–103. (c) Z. Liu, M. Li, D. Cui,

- J. Fei, *J. Controlled Release*, **2005**, *102*, 699–710. (d) C. Rudolph, C. Plank, J. Lausier, U. Schillinger, R. H. Müller, J. Rosenecker, *J. Biol. Chem.*, **2003**, *278*, 11411–11418.
- [18] (a) G. Ruan, A. Agrawal, A. I. Marcus, S. Nie, *J. Am. Chem. Soc.*, **2007**, *129*, 14759–14766. (b) V. Kersemans, B. Cornelissen, *Pharmaceuticals*, **2010**, *3*, 600–620.
- [19] (a) L. Pan, Q. He, J. Liu, Y. Chen, M. Ma, L. Zhang, J. Shi, *J. Am. Chem. Soc.*, **2012**, *134*, 5722–5725. (b) A. Nori, K. D. Jensen, M. Tijerina, P. Kopečková, J. Kopeček, *Bioconjugate Chem.*, **2003**, *14*, 44–50. (c) K. S. Rao, M. K. Reddy, J. L. Horning, V. Labhasetwar, *Biomaterials*, **2008**, *29*, 4429–4438. (d) S. Al-Taei, N. A. Penning, J. C.; Futaki, S. Simpson, T. Takeuchi, I. Nakase, A. T. Jones, *Bioconjugate Chem.*, **2006**, *17*, 90–100.
- [20] Y. Demizu, M. Oba, K. Okitsu, H. Yamashita, T. Misawa, M. Tanaka, M. Kurihara, S. H. Gellman, *Org. Biomol. Chem.*, **2015**, *13*, 5617–5620.
- [21] N. Tamilarasu, I. Huq, T. M. Rana, *Bioorg. Med. Chem. Lett.*, **2001**, *11*, 505–507.
- [22] T. M. Rana, I. Huq, *US Patent 5843995*, **Dec. 1, 1998**.
- [23] W. L. Zhu, S. Y. Shin, *J. Pept. Sci.*, **2009**, *15*, 345–352.
- [24] S. Piantavigna, G. A. McCubbin, S. Boehnke, B. Graham, L. Spiccia, L. L. Martin, *Biochim. Biophys. Acta*, **2011**, *1808*, 1811–1817.
- [25] L. Bourré, F. Giuntini, I. M. Eggleston, C. A. Mosse, A. J. MacRobert, M. Wilson, *Photochem. Photobiol. Sci.*, **2010**, *9*, 1613–1620.
- [26] H. J. Jung, K.-S. Jeong, D. G. Lee, *J. Microbiol. Biotechnol.*, **2008**, *18*, 990–996.
- [27] H. Wang, K. Xu, L. Liu, J. P. K. Tan, Y. Chen, Y. Li, W. Fan, Z. Wei, J. Sheng, Y.-Y. Yang, L. Li, *Biomaterials*, **2010**, *31*, 2874–2881.
- [28] H. Jung, Y. Park, K. Hahm, D. Lee, *Biochem. Biophys. Res. Commun.*, **2006**, *345*, 222–228.
- [29] A. K. Marr, W. J. Gooderham, R. E. Hancock, *Curr. Opin. Pharmacol.*, **2006**, *6*, 468–472.
- [30] N. Wiradharma, U. Khoe, C. A. E. Hauser, S. V. Seow, S. Zhang, Y.-Y. Yang, *Biomaterials*, **2011**, *32*, 2204–2212.
- [31] M. N. Alekshun, S. B. Levy, *Cell*, **2007**, *128*, 1037–1050.
- [32] N. P. Chongsiriwatana, J. A. Patch, A. M. Czyzewski, M. T. Dohm, A. Ivankin, D. Gidalevitz, R. N. Zuckermann, A. E. Barron, *Proc. Natl. Acad. Sci. U.S.A.*, **2008**, *105*, 2794–2799.
- [33] M. D'Costa, V. A. Kumar, K. N. Ganesh, *Org. Lett.*, **1999**, *1*, 1513–1516.
- [34] (a) K. M. Patil, R. J. Naik, M. Vij, A. K. Yadav, V. A. Kumar, M. Ganguli, M. Fernandes, *Bioorg. Med. Chem. Lett.*, **2014**, *24*, 4198–4202. (b) K. M. Patil, *Ph. D. Dissertation*, Pune University, India, **2014**.
- [35] H. Chilukuri, Y. M. Kolekar, G. S. Bhosle, R. K. Godbole, R. S. Kazi, M. J. Kulkarni, M. Fernandes, *RSC Adv.* **2015**, *5*, 77332–77340.
- [36] E. P. Loret, P. Georgel, W. C. Johnson Jr., P. S. Ho, *Proc. Natl. Acad. Sci. USA*, **1992**, *89*, 9734–9738.
- [37] N. J. Greenfield, *Nat. Protocols*, **2007**, *1*, 2876–2890.
- [38] X. Su, X. Zhou, Z. Tan, C. Zhou, *Biopolymers*, **2017**, *107*, e23041; <https://doi.org/10.1002/bip.23041>.
- [39] Y. Chen, M. T. Guarnieri, A. I. Vasil, M. L. Vasil, C. T. Mant, R. S. Hodges, *Antimicrob. Agents Chemother.*, **2007**, *51*, 1398–1406.
- [40] J. V. Olsen, S.-E. Ong, M. Mann, *Mol. Cell. Proteomics*, **2004**, *3*, 608–614.
- [41] K. Midorikawa, K. Ouhara, H. Komatsuzawa, T. Kawai, S. Yamada, T. Fujiwara, K. Yamazaki, K. Sayama, M. A. Taubman, H. Kurihara, K. Hashimoto, M. Sugai, *Infect. Immun.*, **2003**, *71*, 3730–3739.
- [42] U. Singh, S. Akhtar, A. Mishra, D. Sarkar, *J. Microbiol. Methods*, **2011**, *84*, 202–207.

Highlights

- Non-natural lysine and arginine surrogates in Tat(48-57).
- Increased resistance to enzymatic proteolysis.
- Good anti-bacterial activity-MICs between 0.61 to 1.26 μM for γTatM4 .
- MICs 6.6 & 6.0 μM for $\gamma\text{TatM4wg}$ & αTatM3 respectively against dormant *M. tuberculosis*.
- Very low cytotoxic effect on mammalian cells.